Simulation-based Approach to Investigate the Electric Scooter Rider Protection During Traffic Accidents

December 2023 | Final Report

SAFE-D
SAFETY THROUGH DISRUPTION

Texas A&M Transportation Institute

San Diego State University
Leadership Starts Here

VT | Virginia Tech Transportation Institute
Virginia Tech

Disclaimer

The contents of this report reflect the views of the authors, who are responsible for the facts and the accuracy of the information presented herein. This document is disseminated in the interest of information exchange. The report is funded, partially or entirely, by a grant from the U.S. Department of Transportation's University Transportation Centers Program. However, the U.S. Government assumes no liability for the contents or use thereof.

TECHNICAL REPORT DOCUMENTATION PAGE

1. Report No. 05-116	2. Government Accession No.	3. Recipient's Catalog No.
4. Title and Subtitle Simulation-based approach to investigate the electric scooter rider protection during traffic accidents		5. Report Date December 2023 6. Performing Organization Code:
7. Author(s) Costin D. Untaroiu Alexandrina Untaroiu Rafael Chontos Daniel Grindle		8. Performing Organization Report No. Report 05-116
9. Performing Organization Name and Address: Safe-D National UTC Virginia Polytechnic Institute and State University		10. Work Unit No. 11. Contract or Grant No. 69A3551747115/[05-116]
12. Sponsoring Agency Name and Address Office of the Secretary of Transportation (OST) U.S. Department of Transportation (US DOT)		13. Type of Report and Period Final Research Report 10/2020-12/2023 14. Sponsoring Agency Code

15. Supplementary Notes
This project was funded by the Safety through Disruption (Safe-D) National University Transportation Center, a grant from the U.S. Department of Transportation – Office of the Assistant Secretary for Research and Technology, University Transportation Centers Program.

16. Abstract
The recent emergence of electric scooter (e-scooter) rideshare companies has greatly increased the use of e-scooters around the world, which has increased the number of injuries associated with their use. A primary cause of e-scooter crashes is front-wheel collisions with a vertical surface. This research numerically simulated various e-scooter-stopper crashes across different impact speeds, approach angles, and stopper heights to characterize their influence on rider injury risk during falls. A finite element (FE) model of a standing Hybrid III anthropomorphic test device was used as the rider. The angle of approach was found to have the greatest effect on injury risk to the rider. Additionally, arm bracing was shown to reduce the risk of serious injury in two thirds of the impact scenarios. Most e-scooter rider fatalities are recorded in collisions between a car and an e-scooter. Therefore, crashes between an e-scooter and a sedan and between an e-scooter and a sports utility vehicle were simulated using FE models. The vehicles impacted the e-scooter at a speed of 30 km/hr in a perpendicular collision and at 15° towards the vehicle. The risks of serious injury to the rider were low for the head, brain, and neck, but femur/tibia fractures were observed in all simulations.

17. Key Words Electric scooter, rider protection, Impact Simulation, Traffic accidents, LS-DYNA	18. Distribution Statement No restrictions. This document is available to the public through the Safe-D National UTC website, as well as the following repositories: VTechWorks, The National Transportation Library, The Transportation Library, Volpe National Transportation Systems Center, Federal Highway Administration Research Library, and the National Technical Reports Library.

19. Security Classif. (of this report) Unclassified	20. Security Classif. (of this page) Unclassified	21. No. of Pages 22	22. Price $0

Form DOT F 1700.7 (8-72) Reproduction of completed page authorized

Abstract

The recent emergence of electric scooter (e-scooter) rideshare companies has greatly increased the use of e-scooters around the world, which has increased the number of injuries associated with their use. A primary cause of e-scooter crashes is front-wheel collisions with a vertical surface. This research numerically simulated various e-scooter-stopper crashes across different impact speeds, approach angles, and stopper heights to characterize their influence on rider injury risk during falls. A finite element (FE) model of a standing Hybrid III anthropomorphic test device was used as the rider. The angle of approach was found to have the greatest effect on injury risk to the rider. Additionally, arm bracing was shown to reduce the risk of serious injury in two thirds of the impact scenarios. Most e-scooter rider fatalities are recorded in collisions between a car and an e-scooter. Therefore, crashes between an e-scooter and a sedan and between an e-scooter and a sports utility vehicle were simulated using FE models. The vehicles impacted the e-scooter at a speed of 30 km/hr in a perpendicular collision and at 15° towards the vehicle. The risks of serious injury to the rider were low for the head, brain, and neck, but femur/tibia fractures were observed in all simulations.

Acknowledgments

High-performance computing resources of Virginia Tech (VT) - Advanced Research Computing (ARC) were utilized to run the computer simulations. The Hybrid III standing finite element model was provided by LSTC-ANSYS. The human standing (pedestrian) finite element model was provided by the Global Human Body Models Consortium (GHBMC).

This project was funded by the Safety through Disruption (Safe-D) National University Transportation Center, a grant from the U.S. Department of Transportation – Office of the Assistant Secretary for Research and Technology, University Transportation Centers Program.

Special thanks are extended to Dr. Warren Hardy, who served as the subject matter expert and reviewed and provided suggestions for the successful completion of this report.

Table of Contents

List of Figures

List of Tables

Introduction

Since 2012, rideshare companies in the United States have offered standing two-wheel electric scooters (e-scooters) for public short-term rental [1]. Various companies allow people to rent out e-scooters for commuting or recreation, thereby eliminating the need for the population to purchase, store, and maintain a scooter themselves. Despite being relatively new, these rideshare companies have quickly increased the popularity, use, and availability of e-scooters [1-3].

The increase in e-scooter use has also led to an increase in e-scooter traffic injuries [2]. The injuries observed were generally mild to moderate in severity and occurred most frequently to the head and limbs [1-4]. The most common types of injuries to the body were fractures, dislocations, and contusions [1, 3, 5, 6]. From the available literature, the most common mode of crash appeared to be falls, and the most dangerous mode was e-scooter vehicle crashes [3, 5, 7, 8]. A Los Angeles, California-based study found that 80.2% of injuries were caused by falls [3]. The same study also found that collision with an object caused 11% of crashes and collision with a vehicle or other moving object caused 8.8% of crashes [3]. Similarly, a Swedish study found that 83% of scooter crashes involved only the scooter rider, and 12% involved other road users, such as cars or other scooter riders [7]. While vehicle collisions account for a relatively small portion of e-scooter crashes, 80% of rider fatalities were caused by vehicle collisions [9].

The field of e-scooter injury research is relatively new and limited, especially regarding computational crash recreation. Much of the current literature focuses on observing injury trends reported by emergency rooms, but not the biomechanical causes of these injuries. Experimental and modeling-based research on the topic is sparse and has only examined either pothole-based falls [10] or rigid body impacts where the scooter-rider drove into a stationary vehicle [11]. While these studies are insightful, they used rigid-body rider models and were limited in their selection of pre-impact variables. Specifically, the researchers in the pothole impact study recommended varying the angle of approach because their study only used head-on collision scenarios [10]. Notably, neither study investigated how an attempt by the rider to catch themselves might change the injury risks [10, 11].

Additionally, researchers from Knoxville, Tennessee, reported that 67% of collisions between an e-scooter and an automobile occurred at an intersection [12]. Despite this prevalence of impacts, only one study has investigated the biomechanics of this impact scenario. A previous computational study examined a sedan laterally impacting a stationary scooter rider [13]. While this study was insightful, it used an un-validated vehicle model to impact the rider model, it did not examine the injuries from the rider-ground interaction, and the only variable altered was the posture of the rider. To better investigate rider safety, further impact simulations need to be completed using robustly validated vehicle models and a wider variety of impact conditions. Therefore, in addition to a comprehensive literature review [14], the current researchers performed two main studies: a numerical investigation of rider injury risks during falls caused by e-scooter

stopper impacts (the main cause of e-scooter rider injuries) [15] and a numerical investigation of e-scooter-to-vehicle traffic accidents (the main cause of e-scooter rider fatalities) [14]. All of these efforts were included in a Master of Science thesis presented to the Department of Biomedical Engineering and Applied Mechanics at Virginia Tech as well [14].

Numerical Investigation of Rider Injury Risks During Falls Caused by E-scooter Stopper Impacts

The objective of this study [15] was to investigate the biomechanical causes of trauma associated with e-scooter crashes resulting in fall events across a range of pre-impact conditions. These falls were created by numerically simulating a rider falling off an e-scooter after impacting a vertical transition referred to as a "stopper" (i.e., curb or another rigid object). To investigate this event, a finite element (FE) model of an e-scooter was developed and the Hybrid III model (HIII), an anthropometric test device (ATD) currently used in automotive impact regulations, acted as an e-scooter rider to simulate falls. This study is among the first to use a deformable rider model to explore the effect of various e-scooter pre-impact conditions and their effect on rider safety; this study also lay the foundation for further e-scooter fall research.

Numerical Investigation of E-scooter-to-Vehicle Traffic Accidents

The objective of this study [14] was to investigate the biomechanical causes of rider injuries in intersection vehicle impacts across a range of pre-impact conditions using FE models. This study is among the first to use a deformable rider model and validated vehicle model to investigate rider injury risks and expand the knowledge of vehicle-rider injury outcomes.

Numerical Investigation of Rider Injury Risks During Falls Caused by E-scooter Stopper Impacts

Methods

To investigate e-scooter crashes, models of an e-scooter, a road, and a stopper were created. The three pre-impact variables examined in this study were impact speed, stopper height, and approach angle. Additionally, the simulations that modeled a head-on collision were run a second time with arm muscle activation to simulate a rider attempting to catch themselves to break the fall.

Development of an E-scooter FE Model

The scooter geometry was created by scanning a Spin (SPIN, San Francisco, CA) Ninebot KickScooter MAX e-scooter using a FARO laser scanner system [15]. The initial geometry was smoothed and transformed into a non-uniform rational B-spine (NURBS) surface in Rhino 3D (Robert McNeel & Associates, Seattle, WA) and then imported to be meshed in Hypermesh (Altair, Troy, MI). Finally, the scooter mesh was imported into LS-PrePost (LSTC/Ansys, Cannonsburg, PA), where the scooter parts were defined and their material properties assigned

based on data from the literature (Figure 1). In this model, all parts of the scooter were rigid except for the tires.

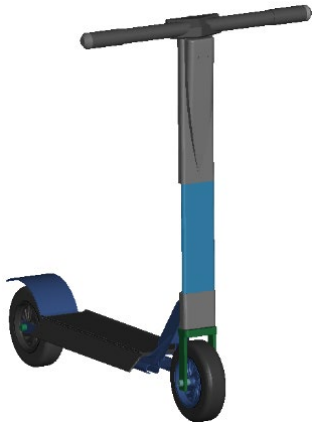

Figure 1. Computer model. Spin e-scooter FE rendering.

The e-scooter tire shells were modeled using a piecewise linear plasticity material and inflated like an airbag [16]. The scooter was connected with 13 rigid body constraints and two joint revolute constraints. The two joint revolute constraints were used on the rods that connect the front tire to the front arm and the rear tire to the deck to allow the rods to spin with the tires. The wheel supports were in between the tire shell and the rims. The e-scooter was 1,110 mm tall and 1,008 mm in length. The deck of the scooter was 536 mm by 205 mm, and the handlebars had a 680-mm span. The wheels had an inner radius of 69 mm, an outer radius of 111 mm, and a thickness of 60 mm.

E-scooter-Stopper Impact Simulations

To model an e-scooter crash, the calibrated HIII FE model was placed on the e-scooter model (Figure 2). The hands and feet were constrained to the scooter using the COONSTRAINED_JOINT_LOCKING keyword card [17]. The release times of the feet and hands were adjusted based on the time of impact between the scooter and the stopper. The feet and hands were released 6 ms after the moment of the wheel-stopper impact. The ground was modeled as a deformable asphalt structure using the LS-Dyna material card 159 MAT_CSCM_CONCRETE [18]. The contact between the ATD and the ground was modeled using the automatic_surface_to_surface contact card [17] with the soft contact option 1. Additionally, the static coefficient of friction was set as 0.85, and the dynamic coefficient was set as 0.6.

A design of experiments (DOE) study was used to investigate the effect of impact speed, stopper height, and approach angle on rider injury risks. The impact speeds used in this study were 3.2 m/s, 4.48 m/s, and 11.16 m/s. These speeds were chosen based on the reported operation speeds of e-scooters [19]. The linear velocity of the scooter and ATD was achieved using initial velocity generation and initial velocity rigid body keyword cards. Both the ATD and the scooter were given the same initial linear velocity. An angular velocity was applied to the wheels of the scooter using initial velocity keyword cards. This made the wheels spin as they would on a moving scooter. The stopper heights examined were 52 mm, 101 mm, and 152 mm. The first two stopper heights were

chosen to simulate the scooter impacting small obstacles or bumps (Figure 2a) that are sometimes present on the sidewalks, bike lanes, and streets on which e-scooters are typically operated [5, 20, 21]. The last stopper height was selected because 152 mm is the height of a typical curb [22]. The ground on the other side of the 152-mm stopper was raised to mimic how the ground after a curb is generally higher than the street (Figure 2b).

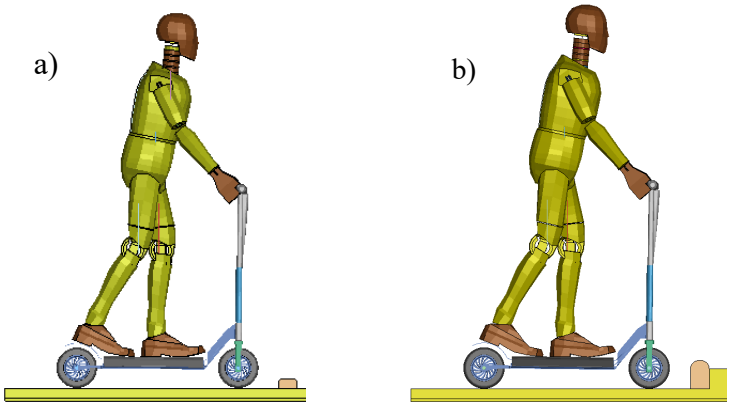

Figure 2. Computer models. The scooter setup for a stopper height of 52 mm and an approach angle of 90° (a) and a stopper height of 152 mm and an approach angle of 90° (b).

Finally, the approach angles tested were 90°, 60°, 45°, and 30°. The approach angle was the angle between the line of travel of the scooter and the obstacle (Figure 3). A Latin hypercube scheme was used to generate 36 crash scenarios.

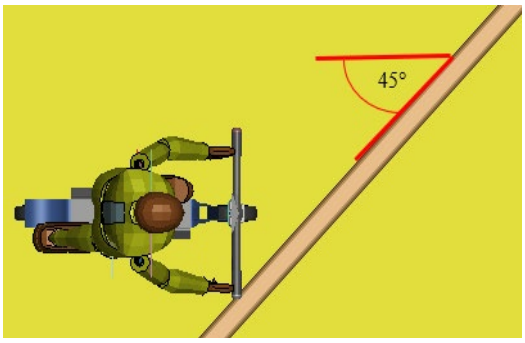

Figure 3. Computer model. The initial setup for a 45° approach angle.

Nine additional simulations were run using a perpendicular initial collision configuration (90° approach angle). In these additional simulations, the HIII was modeled attempting to break its fall with its hands extended forward. To simulate arm activation, the ATD's shoulder and elbow joints were loaded directly after the wheel-stopper impact, which caused the arms to rotate forward simulating a rider trying to catch themselves with their hands (Figure 4). The results from the arm activation simulations were directly compared to the same simulations without arm activation to observe how the arm activation affected the risk of injury.

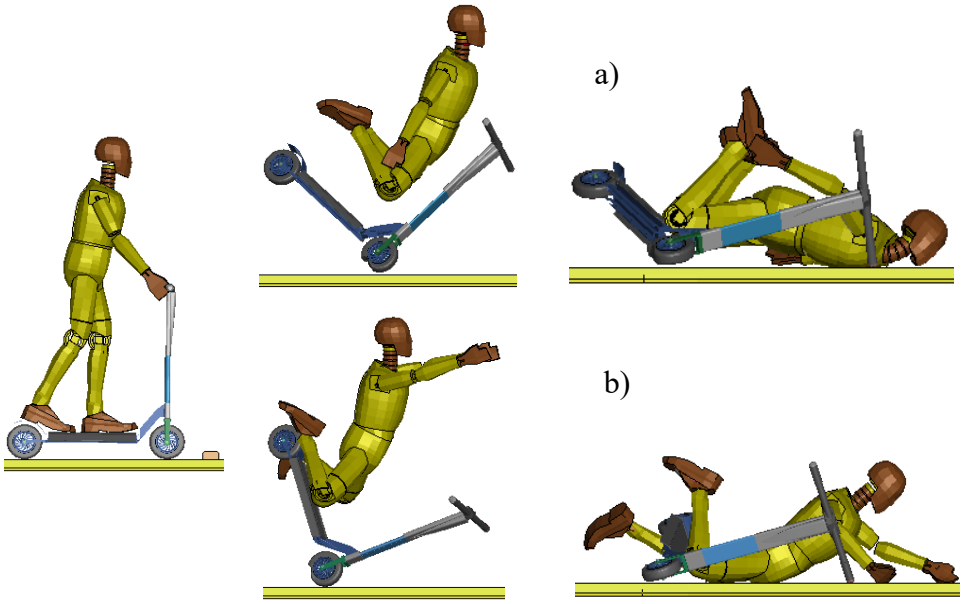

Figure 4. Computer models. The ATD falling without arm activation (a) and with arm activation (b).

Risk probabilities of serious body region injuries (Abbreviated Injury Scale score of 3 or more [AIS 3+]) were calculated based on head injury criteria (HIC), neck injury criteria (NIC), chest deflection, and maximum femur force [23]. These probabilities were used to calculate the rider injury measure (RIM) as an overall likelihood of serious injury to the rider (Table 1). The brain injury criteria (BrIC) was not examined in this study because the presence of evidence of traumatic brain injury in scooter crash patients was 15% or lower [2, 21, 24], and the HIII ATD has not been tested for BrIC outcomes.

Table 1. Injury Risk Functions (AIS 3+)

Injury metrics	Risk Function	Ref
HIC_{15}	$P_{HIC} = \Phi\left(\frac{\ln(HIC_{15}) - 7.45231}{0.73998}\right)$	[23]
N_{ij}	$P_{N_{ij}} = \frac{1}{1 + e^{3.227 - 1.969 * N_{ij}}}$	[25]
Chest Deflection	$P_{chest} = \frac{1}{1 + e^{10.5456 - 1.568 * (\delta_{max})^{0.4612}}}$	[23]
Femur Compression	$P_{femur} = \frac{1}{1 + e^{4.9795 - 0.326 * FemurForce}}$	[23]
RIM	$1 - (1 - P_{HIC}) * (1 - P_{BrIC}) * \left(1 - P_{N_{ij}}\right) * (1 - P_{chest}) * (1 - P_{femur})$	[23]

The Pearson product-moment correlation coefficients between DOE variables and the probability of injuries were calculated to measure the strength of the relationship between different crash pre-impact conditions and injury risks. The correlation coefficients were calculated by importing the pre-impact conditions and resulting injury risks from each simulation into LS-Opt. In addition, the global effects of each pre-impact variable on the risk of injury were examined using Sobol's global sensitivity analysis in LS-Opt [26]. When combined with the information obtained from the

correlation coefficient, the sensitivities provided insight into which variables had the largest impact on rider injury. Student *t*-tests were calculated to determine if arm activation caused statistically significant changes in injury outcomes. In this statistical test, called also null-hypothesis significance testing (NHST), a *p*-value is calculated, and if $p \leq \alpha = 0.05$ [27], it is typically considered to be statistically significant (the null hypothesis is rejected). However, it should be mentioned that NHST has several shortcomings [28], so NHST tests can only be considered preliminary (exploratory) heuristics [28]. The simulation set that used a head-on impact with a stopper height of 52 mm and impact speed of 3.2 m/s was excluded from the *t*-tests because it was an outlier [29].

Results

The final e-scooter model contained a total of 392,450 elements and 387,966 nodes. All of the scooter parts except for the tire shells were modeled using a rigid material model for steel [14].

A wide range of RIM scores—ranging from 0.08 to 1.0 (Table 3)—were observed across the simulations. In concurrence with reported injuries, the most injured body regions were the head and neck [1-3]. Notably, in 10 of the 11 simulations that reported RIM > 0.9, HIC was the largest regional injury measure and typically by a large margin. Head injury AIS 3+ risks were above 25% in 16 out of 36 simulations. Neck injury risks were above 25% in 18 out of 36 simulations. Chest injury risks were above 25% in 2 of the 36 simulations. Femur injury risks were below 25% in all simulations.

Approach angle had the largest influence on all four injury outcomes, reporting 56% to 91% of sensitivities (Figure 5a). The correlation coefficients, determined using the analysis of variance (ANOVA), a linear sensitivity measure implemented in LS-Opt, indicated that larger approach angles were strongly correlated with larger head (0.602), neck (0.615), chest (0.648), and overall (0.627) injury risks (Figure 5b). Approach angle had a small negative association with the risk of femur injury (-0.19). Four of the five lowest RIM simulations used the smaller approach angles of 30° and 45°. Furthermore, nearly all the simulations with a RIM of 1.0 used a 90° approach angle.

Impact speed had the second largest effect on injury measures, with sensitivity values between 5% and 30%. Impact speed was slightly negatively correlated with RIM (-0.025) and chest injury (-0.062), but positively correlated with head (0.066), neck (0.121), and femur (0.263) injury. Speed had the largest effect on femur injury risks even though femoral injury risk never rose above 21.7%.

Stopper height had the smallest effect on injury measures, with sensitivity values between 3% and 16%. Stopper height had a moderately negative correlation with RIM (-0.307), suggesting that larger heights reported smaller RIM values (Figure 5b). Stopper height was negatively correlated with head (-0.205) and neck (-0.073) injury risks but was positively correlated with femur (0.144) and chest (0.045) injury risks.

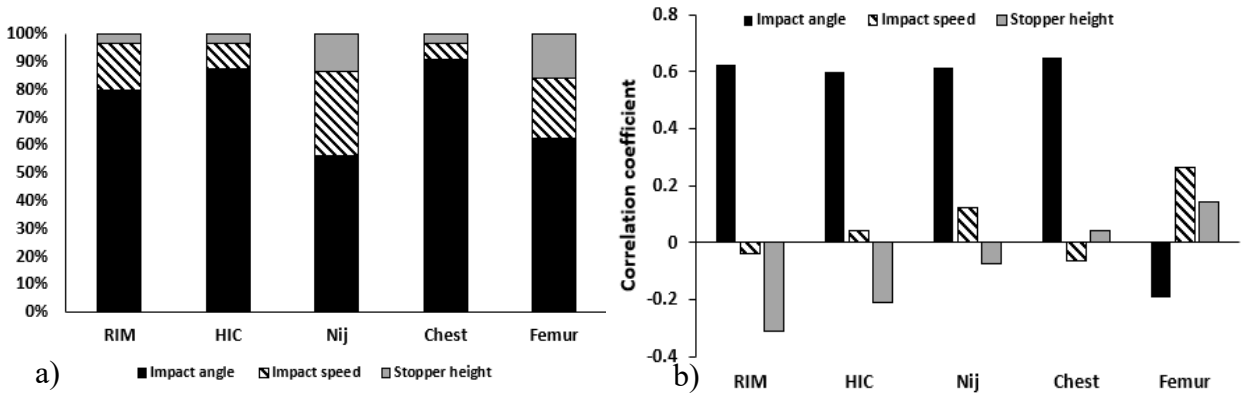

Figure 5. Graphs. Sensitivity of injury risks to pre-impact variables global sensitivity approach/Sobol (a) and linear sensitivity approach/ANOVA (b).

ATD arm activation caused varying effects on injury risks (Table 4). Six of the nine simulations resulted in reduced RIM scores when arms were activated. RIM typically decreased because of lower head, neck, and chest injury risks. ATD arm activation had a statistically significant effect on neck injury risk ($p = 0.042$); the effects on RIM ($p = 0.065$) and HIC ($p = 0.064$) injury risk were not statistically significant, though the p-values were much closer to the significance level than for the effects on chest ($p = 0.119$) and femur ($p = 0.32$) injury risk, which were also not significant.

Discussion

This study is among the first to examine e-scooter falls with a deformable rider model and a variety of pre-impact conditions. In addition to the development of an FE e-scooter, an FE model of the HIII pedestrian was calibrated. The calibrated HIII showed responses in the corridors of certification tests, suggesting the ATD model can be used by the safety community in car-to-pedestrian simulations.

Compared to a recent study performed to investigate the falls of e-scooter riders caused by potholes [10], this study investigated a larger group of speeds and different stopper heights, and it considered possible rider arm activation during contact with the ground. Furthermore, the current study included the angle of approach as a variable, which had a significant effect on RIM. Finally, an FE approach was used, which has more accurate contact modeling compared to the rigid-body approach used by other groups [10]. Another recent study used various angles of approach; however, that study focused mainly on the head and compared the risk of severe head injuries for a rider wearing a helmet and a rider without a helmet [30]. In contrast, the current study observed injuries across the entire ATD and specifically looked at how changing the angle of approach and arm activation affected the fall kinematics and RIM.

The pre-impact condition with the largest impact on rider injury risk was the angle of approach. Perpendicular impacts (90°) reported substantially larger injury risks than impacts at 30° to 60°. Impact speed and stopper height, in the ranges investigated in this study, played small roles in

injury risk outcomes. The surprisingly low correlation of the scooter speed with head/RIM injury risk may be partially explained because the injuries are caused mostly by the vertical head impact with the ground (caused by gravity), not by the horizontal velocity. Similar findings have been observed for pedestrian ground contact injuries [31]. The recorded RIM values varied between 0.08 and 1.0. About half of the RIM scores indicated a high risk of serious injury to the rider despite many reported injuries resulting from e-scooter use being mild to moderate in severity. This was not surprising, as the speeds tested were in the upper 25th percentile for reported e-scooter usage speeds [19].

Approach angle may have had the largest effect on injury measures because the angle of approach largely determined how the rider fell and which parts of the body hit the ground first. In a 90° impact, the ATD fell or flew forward. For example, in the high-speed 90° impact, the flung ATD's head hit the ground first, resulting in large HIC and RIM values (Figure 6). In the lower speed 90° impacts, the knees hit the ground first, and the ATD collapsed forward with the chest and head contacting the ground at high angular velocities. In contrast, an approach angle of 30° caused the rider to land on their side and shoulder first. In most cases, the head of the HIII ATD did not contact the ground at all, resulting in a lower HIC and RIM (Figure 7). RIM did not increase in these shoulder-first impacts because only anterior-posterior chest deflection was examined, and thus any risk of lateral chest deflection-based injuries was not incorporated.

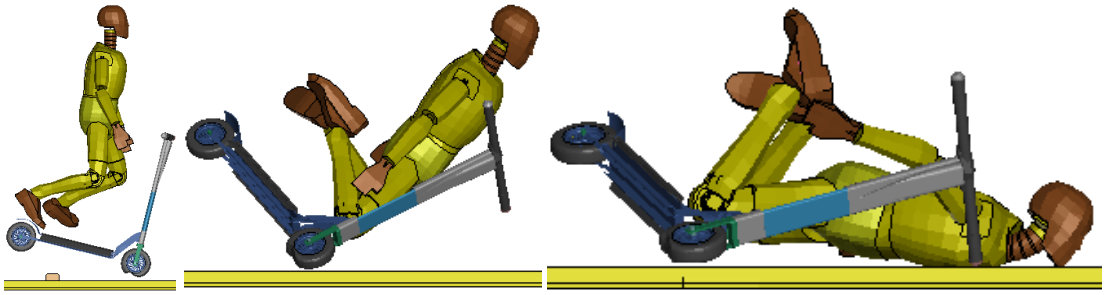

Figure 6. Computer model. 90° approach angle, 52 mm stopper, 11.16 m/s impact without arm activation.

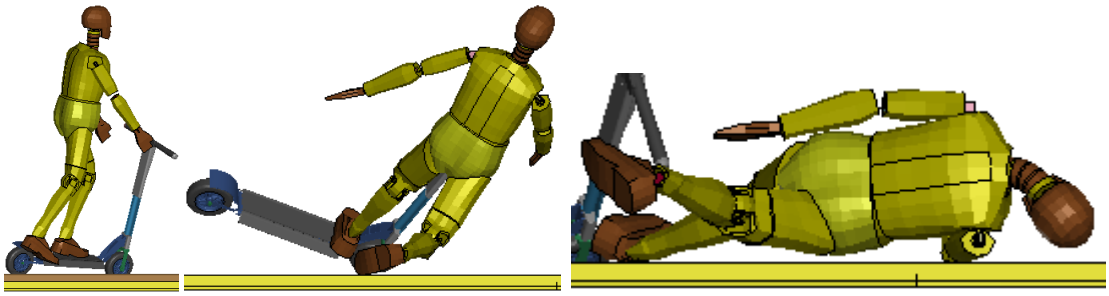

Figure 7. Computer model. 30° approach angle, 52 mm stopper, 11.16 m/s impact without arm activation.

A surprising result of the study was the small and negative correlation between impact speed and RIM. However, when the simulations were grouped such that speed was the only variable changed in each group (Table 4), a trend emerged between the sign of the correlations and the angle of

approach for the group. For angles of attack of 60° and 90°, impact speed had a primarily positive correlation with injury risk. For angles of attack of 45° and 30°, impact speed had a primarily negative correlation with injury risk. This trend could be attributed to the angle of approach changing the kinematics of the fall. For collisions involving higher angles of approach, the ATD landed with its chest and head facing the ground, and speed had the expected positive correlation with injury risk. However, for smaller angles of approach, the ATD landed primarily on its side where little to no injury risks were observed. Thus, the direction the ATD impacted the ground may have played a larger role in impact outcomes than speed.

Interestingly, the ATD attempting to catch itself did not reduce the risk of serious injury as much as initially expected. This was primarily caused by the kinematics of the fall varying between each simulation and the ATD being unable to mimic exactly how a person would respond while falling. For example, in the case of a head-on collision with a 52 mm stopper at 3.2 m/s and arm activation, the ATD catches itself and then bounces before eventually having its head contact the ground, resulting in large HIC values (Figure 8). In this specific case, the HIC is higher than the no-arm activation case, causing the RIM to increase. However, a person may not have impacted the ground after successfully catching themselves or may have adjusted their arms to brace for the second impact. A scenario such as this might cause a greater reduction of the risk of injury to the neck and head regions, which were usually the biggest contributors to the RIM for the rider. Because of the unusually large increase in RIM, this specific simulation set was excluded from the I-test calculation.

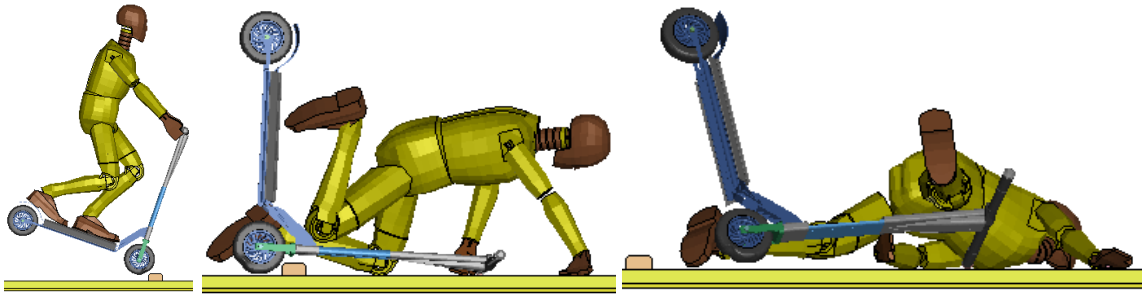

Figure 8. Computer model. 90° approach angle, 52 mm stopper, 3.2 m/s impact with arm activation.

This study was limited in its selection of injury measures. The RIM equation only examined head, neck, anterior-posterior chest, and femoral injury risks. This technique excluded potential injuries caused by lateral-medial chest compression. Not including this injury measure caused the chest injury risk for simulations where the ATD landed on its side to be unrealistically small since only anterior-posterior deflection was examined (Figure 7). In addition, upper extremity injuries were not examined in this study despite being reported in e-scooter falls. These injury measures were excluded because the HIII ATD model had not been calibrated for these loading scenarios. Future work should use a rider model that can better capture more injury measures to further explore e-scooter falls. For example, replacing the coarse HII FE model with a detailed or simplified human pedestrian FE model (e.g., Global Human Body Models Consortium [GHBMC], Total Human

Model for Safety [THUMS]) [32-34], which include more impact validations (e.g. in a lateral plane), may provide more biofidelic responses and should be investigated in the future. The rider's kinematics during the fall phase may be influenced significantly by the wheel-bumper impact and the time when the rider's hands are disconnected from the scooter handlebars. Therefore, additional validation of the rider-scooter models is recommended when physical collision data are available.

An additional limitation of this study was its impact speed selection. This study only examined impacts with linear initial velocities, while real e-scooter riders experience crashes and falls during turning or braking events. These different initial velocity and acceleration conditions may result in rider kinematics not seen in this study. Future work should examine the turning events and braking events prior to crashes and falls to better investigate e-scooter safety.

Numerical Investigation of E-scooter-to-Vehicle Traffic Accidents

Methods

To investigate scooter-car crashes, a previously developed e-scooter model was acquired [35]. The scooter rider was modeled with the GHBMC simplified 50th percentile male pedestrian model (M50-PS) [36]. The GHBMC M50-PS was selected because it was a more biofidelic pedestrian model than other low-computation options such as the HIII model [29]. The GHBMC was positioned on the e-scooter to mimic a typical e-scooter rider stance (Figure 9) [37].

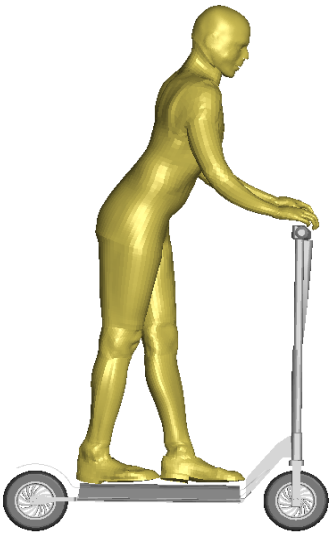

Figure 9. Computer model. The GHBMC model positioned on the scooter.

Two publicly available and validated vehicle models were used to impact the rider, a sedan (FCR) and a sports utility vehicle (SUV) [38]. The two different vehicle types (low profile and high

profile) increased the breadth of potential rider outcomes [38]. The original windshield models were rigid, but this would have created unrealistic rider-windshield interactions; thus, the windshield was made deformable. The deformable windshield was modeled as a dual-layer windshield, with the top layer modeled as glass and the bottom layer modeled as polyvinyl butyral (PVB) [39]. The ground was modeled as deformable asphalt, as in a previous FE rider injury study [35]. An initial linear velocity of 3.2 m/s was applied to the scooter and rider, and the vehicle had an initial speed of 30 km/h with 1 gravity of braking acceleration after the first contact with the rider/e-scooter. The scooter's line of travel was perpendicular to the vehicle's line of travel (Figure 10). Rider position has been examined in previous work, so only a single posture was examined in this study.

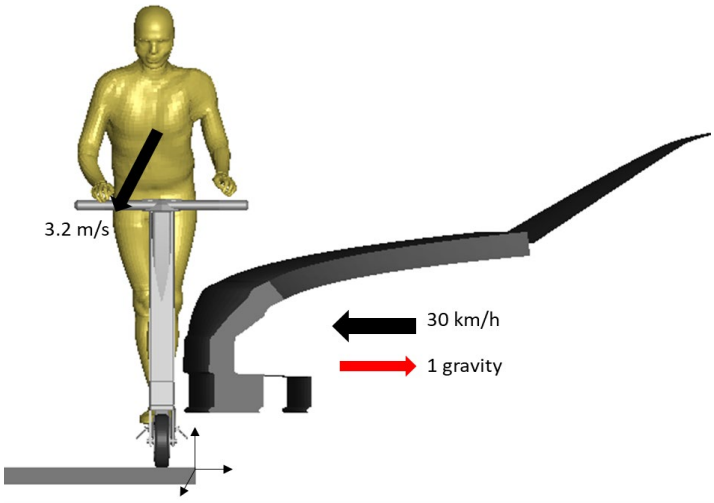

Figure 10. Diagram. The setup of a model of a sedan vehicle impacting the left side of the scooter rider.

There were two primary types of intersection vehicle-rider impacts [12]. The first type was a vehicle traveling straight through the intersection and impacting a rider coming from the motorists' right side [12]. This typology accounted for 31% of intersection collisions [12]. The second common crash type accounted for 29% of intersection collisions and was a motorist turning right at an intersection and a scooter again coming from the right of the motorist [12]. These two impact types were modeled by adjusting the angle of the scooter by 15° to mimic a scooter rider being impacted by a turning vehicle (Figure 11).

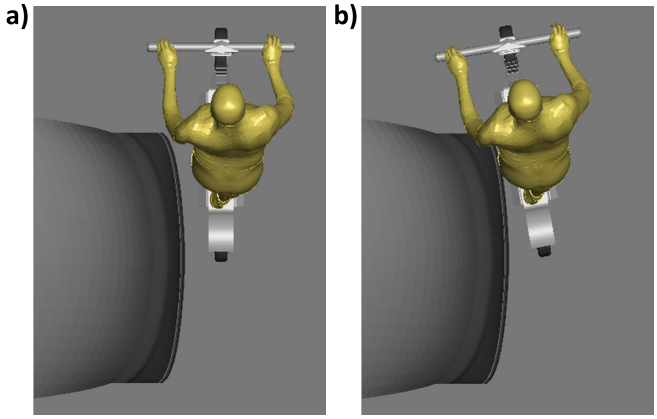

Figure 11. Computer models. A head-on collision (a) and an angle impact collision (b).

The impact simulations were run on the Virginia Tech Advanced Researching Computing cluster in LS-DYNA (version 10.2). Simulations were run until the rider model hit and rested on the ground. The probability of serious injury (AIS 3+) was calculated using injury outcomes from the HIC, BrIC, neck injury risk (N_{ij}), femur injury risk, and tibia fracture risk (Table 2). Lower extremity component failure (element elimination) was permitted in these simulations. If element erosion was observed in the tibia or femur, the injury risk was recorded as 1.

Table 2. Injury Risk Functions (GHBMC M50 FE Model)

Injury metrics	Risk Function	Ref
HIC_{15} (AIS 3+)	$P_{HIC} = \Phi\left(\frac{\ln(HIC_{15}) - 7.45231}{0.73998}\right)$	[23]
BriC (AIS 3+)	$P_{BrIC} = 1 - e^{-\left(\frac{BrIC}{0.987}\right)^{2.84}}$	[23]
N_{ij} (AIS 3+)	$P_{N_{ij}} = \frac{1}{1 + e^{3.227 - 1.969 * N_{ij}}}$	[25]
Femur Fracture Risk	$P_{Femur} = \frac{1}{1 + e^{4.9795 - 0.326 * F}}$	[23]
Tibia Fracture Risk	$P_{Tibia} = \frac{F}{F_c} + \frac{\sqrt{M_x^2 + M_y^2}}{M_c}$	[40]

Results and Discussion

All four impacts reported tibia and femur fractures (Figure 12). The risk of neck injury was low across all the impacts (neck risk < 0.05). Three out of the four impacts reported low head and brain injury risks, but the straight SUV impact reported more substantial risks (head risk = 0.56, brain risk = 0.22).

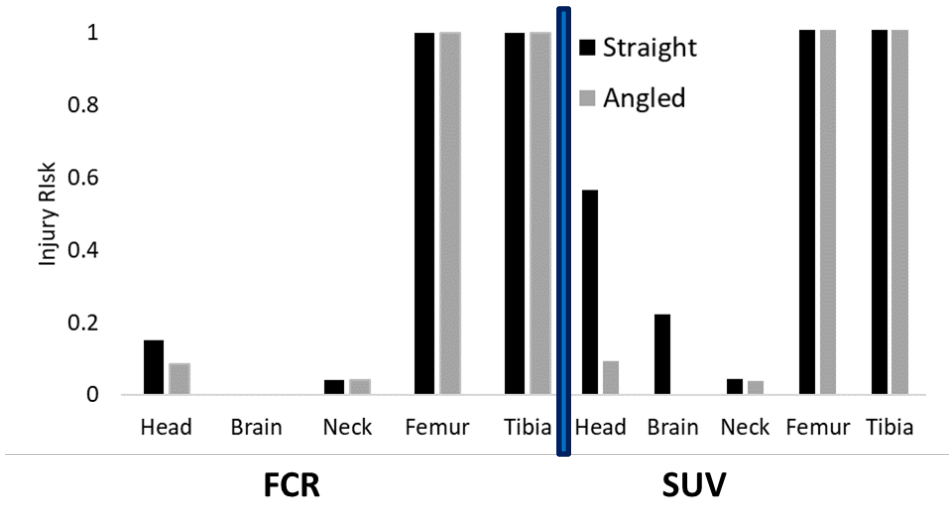

Figure 12. Graphs. Injury risks to the rider based on region.

In three of the four impacts, the head, brain, and neck reported low injury risks due to a lack of head-vehicle or head-ground contact. In these impacts, the rider's head never hit the vehicle; instead, the rider rolled forward and separated from the vehicle (Figure 13). In addition, for these impacts, the rider impacted the ground first with their legs and arms, breaking the fall and reducing the intensity of the head-ground contact. In two impacts, the head never hit the ground due to the arms breaking the fall.

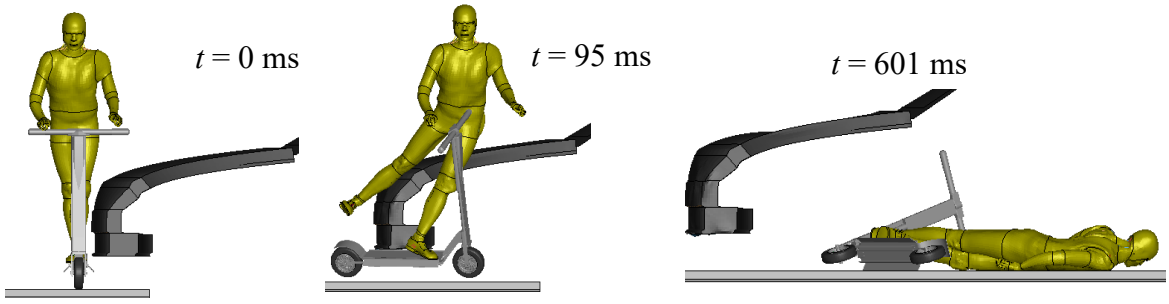

Figure 13. Computer models. Rider kinematics with minimal head injury (FCR-Straight).

The SUV-Straight impact reported larger head and brain injury risks because the rider's head contacted the ground (Figure 14). In this impact, the rider flipped over the hood of the SUV and impacted the ground headfirst, resulting in large head and brain injury risks. These results suggest that to properly protect the rider, the head-ground contact must be softened, and the vehicle impact was not the cause of life-threatening injury.

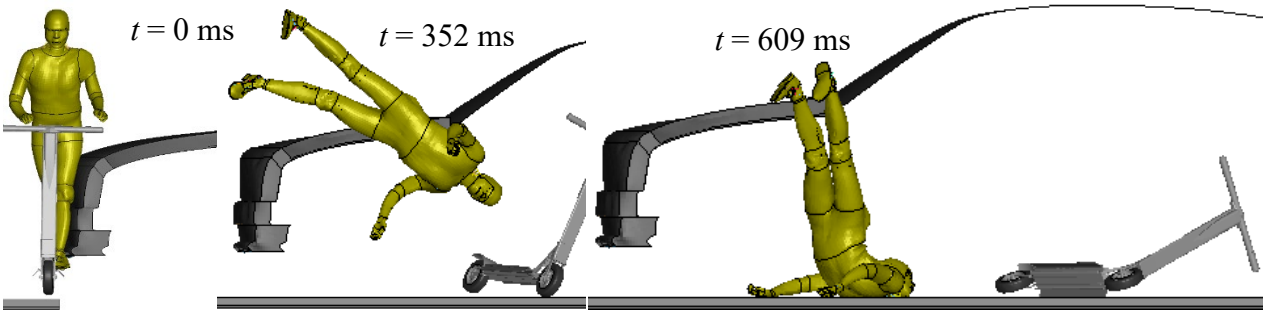

Figure 14. Computer models. Rider kinematics with minimal head injury (SUV-Straight).

The head, brain, and neck injuries reported in this study matched reported rider injuries in vehicle collisions, but the tibia and femur injuries were larger than what was reported in injury surveys [12]. One possible reason for this leg injury discrepancy is that the vehicle impact velocity in most intersection crashes may be lower than what was modeled in this study. It is likely that smaller impact velocities would reduce the risk of serious injuries to the femur and tibia.

This study was limited by its lack of muscle activation. It is likely a rider would attempt to break their fall in an impact. This arm motion and muscle activation may alter the kinematic impact response and potentially change the injury outcomes [29]. For example, shielding of the head may have prevented the large head injury risk in the SUV-Straight impact (Figure 14). Future work should examine the effect of bracing and shielding on impact outcomes.

In addition to a lack of muscle activation, this study was limited in its pre-impact conditions. A single impact speed was explored. To capture a wider range of rider kinematic and injury responses, vehicle impact speed and rider initial velocities should be varied.

Conclusions and Recommendations

Limitations and Future Work

FE models of 50th percentile standing male ATDs were used in this study to exam injury risk to a scooter rider during a variety of crash scenarios. The main limitations of this study were the human model selection, muscle passivity, and injury criterion selection.

Only an FE model of a 50th percentile male was used in this study. Although the median weight for injured riders was about 82 kg, over 20% of rider weighed over 100 kg [5]. Also, 30% to 50% of injured riders were female [1-3, 5, 6, 20, 21, 41]. This shows a gap in the current research, as most studies have focused on male riders. Additionally, height, weight, and sex have been shown to affect injury outcomes in car-pedestrian collisions [42, 43]. Future e-scooter crash studies should use different anthropometries to observe what effect, if any, rider height, weight, and sex have on injury outcomes.

The crash simulations in this study used passive models. Generally, people in real-world scenarios would react to falling or being crashed into. The way a person reacts can affect the injuries they

experience as a rider. The muscle activation used in this project [29] was a rudimentary attempt to model a rider attempting to catch themselves. This muscle activation is a great starting point but should be refined and improved in future studies. Lastly, the simulations in this study focused on the risk of serious injury to the rider and did not look into arm injuries. As arms are one of the most commonly injured regions of the body, future studies should create simulation use rider models capable of outputting arm injury/fracture risk.

Conclusion

In this study, an FE model of a male 50th percentile standing HIII ATD was calibrated and used in scooter-bump crash simulations. A way to model muscle activation was developed and applied to select simulations in scooter-bump collisions. In addition, a simplified FE model of a male 50th percentile GHBMC model was used to model a scooter rider in scooter-car crash scenarios. The results of the scooter-bump simulations showed that, in scenarios where the rider falls off the scooter, the head is the most likely region of the body to be injured. In a scooter-bump scenario, should the rider fail to react to the fall, it was discovered that they would very likely experience serious injuries to the head and neck. The rudimentary arm activation reduced the risk of serious injury to the rider's head and neck, too. Interestingly, the scooter-bump collision showed that for a fall scenario, the angle of approach was the most significant factor in determining the likelihood of serious injury and the location of injury occurrence. The scooter-car impact resulted in serious injuries to the legs of the riders but showed primarily low risks of serious injuries to the head and neck of the rider. The work presented in this study helped link crash mechanisms to injuries, which can be expanded further in future studies.

Additional Products

The Education and Workforce Development (EWD) and Technology Transfer (T2) products created as part of this project can be downloaded from the project page of the Safe-D website. The final project dataset is located in the Safe-D Collection of the VTTI Dataverse.

Education and Workforce Development Products

The EWD products developed as a part of this project are listed below.

- In May 2023, a Virginia Tech graduate student involved in the project successfully defended a Master of Science. graduate thesis based on the subjects developed within the research project. Three journal manuscripts of this research report are published [29] or under review [14] as part of the thesis: Chontos, R., A Numerical Investigation of E-scooter Riders' Injury Crash Mechanisms Using Finite Element Analysis, Master's Thesis, Virginia Tech University, Blacksburg, 2023.

Technology Transfer Products

The T2 products developed as a part of this project are listed below.

- Two presentations related to preliminary results obtained in this project were provided during the Biomedical Engineering Society 2021 Annual Meeting (October 6-9, 2021, Orlando, FL) by R. Chontos and the American Society of Mechanical Engineers (ASME) International Design Engineering Technical Conferences and Computers and Information in Engineering Conference (August 14 – 17, 2022, St. Louis, MO) by Dr. C. Untaroiu.

- One journal paper was accepted to be published in the ASME *Journal of Biomedical Engineering* [29], and two other journal manuscripts [14] are under review.

Data Products

The data products uploaded to the Safe-D collection on the VTTI Dataverse as a part of this project are available on the at Safe-D Collection of the VTTI Dataverse and listed below.

- The HIII standing (rider) model developed by LSTC-Ansys and calibrated by Virginia Tech during this project.

References

[1] Aizpuru, M., Farley, K. X., Rojas, J. C., Crawford, R. S., Moore Jr, T. J., and Wagner, E. R., "Motorized scooter injuries in the era of scooter-shares: a review of the national electronic surveillance system," *The American Journal of Emergency Medicine, 37*(6), 2019, pp. 1133-1138.

[2] Puzio, T. J., Murphy, P. B., Gazzetta, J., Dineen, H. A., Savage, S. A., Streib, E. W., and Zarzaur, B. L., "The electric scooter: A surging new mode of transportation that comes with risk to riders," *Traffic Inj Prev, 21*(2), 2020, pp. 175-178.

[3] Trivedi, T. K., Liu, C., Antonio, A. L. M., Wheaton, N., Kreger, V., Yap, A., Schriger, D., and Elmore, J. G., "Injuries associated with standing electric scooter use," *JAMA Network Open, 2*(1), 2019, pp. e187381-e187381.

[4] Harbrecht, A., Hackl, M., Leschinger, T., Uschok, S., Wegmann, K., Eysel, P., and Müller, L. P., "What to expect? Injury patterns of Electric-Scooter accidents over a period of one year-A prospective monocentric study at a Level 1 Trauma Center," *European Journal of Orthopaedic Surgery & Traumatology, 32*(4), 2022, pp. 641-647.

[5] English, K. C., Allen, J. R., Rix, K., Zane, D. F., Ziebell, C. M., Brown, C. V., and Brown, L. H., "The characteristics of dockless electric rental scooter-related injuries in a large US city," *Traffic Injury Prevention, 21*(7), 2020, pp. 476-481.

[6] Badeau, A., Carman, C., Newman, M., Steenblik, J., Carlson, M., and Madsen, T., "Emergency department visits for electric scooter-related injuries after introduction of an urban rental program," *The American Journal of Emergency Medicine, 37*(8), 2019, pp. 1531-1533.

[7] Stigson, H., Malakuti, I., and Klingegård, M., "Electric scooters accidents: Analyses of two Swedish accident data sets," *Accident Analysis & Prevention, 163*, 2021, p. 106466.

[8] Coelho, A., Feito, P., Corominas, L., Sanchez-Soler, J. F., Perez-Prieto, D., Martinex-Diaz, S., Alier, A., and Monllau, J. C., "Electronic Scooter-Related Injuries: A New Epidemic in Orthopedics," *Journal of Clinical Medicine, 10*(15), 2021.

[9] Santacreu, A., Yannis, G., de Saint Leon, O., and Crist, P., *Safe micromobility*. International Transport Forum, 2020.

[10] Posirisuk, P., Baker, C., and Ghajari, M., "Computational prediction of head-ground impact kinematics in e-scooter falls," *Accident Analysis & Prevention, 167*, 2022, p. 106567.

[11] Ptak, M., Fernandes, F. A. O., Dymek, M., Welter, C., Brodziński, K., and Chybowski, L., "Analysis of electric scooter user kinematics after a crash against SUV," *PLOS ONE, 17*(1), 2022, p. e0262682.

[12] Shah, N. R., Aryal, S., Wen, Y., and Cherry, C. R., "Comparison of motor vehicle-involved e-scooter and bicycle crashes using standardized crash typology," *Journal of Safety Research, 77*, 2021, pp. 217-228.

[13] Bońkowski, T., Špička, J., and Hynčik, L., "On the simulation of electric scooter crash-test with the hybrid human body model," *Proc. 2022 20th International Conference on Emerging eLearning Technologies and Applications (ICETA), IEEE*, 2022, pp. 59-65.

[14] Chontos, R., *A Numerical Investigation of E-scooter Riders' Injury Crash Mechanisms Using Finite Element Analysis*, M.Sc. thesis, Virginia Tech, Blacksburg, VA, 2023.

[15] Chontos, R., Grindle, D., Untaroiu, A., Doerzaph, Z., and Untaroiu, C., "A Numerical Investigation of Rider Injury Risks During Falls Caused by E-Scooter-Stopper Impacts," *J Biomech Eng, 145*(10), 2023.

[16] Marzougui, D., Samaha, R. R., Cui, C., Kan, C.-D., and Opiela, K. S. Extended Validation of the Finite Element Model for the 2010 Toyota Yaris Passenger Sedan, No. NCAC 2012-W-005. Presented at 92nd Annual Meeting of the Transportation Research Board, Washington, D.C., 2013: https://trid.trb.org/view/1241559

[17] LSTC, *LS-Dyna Keyword User's Manual*, 2017.

[18] LSTC, *LS-Dyna Keyword User's Manual, Material Models*, 2017.

[19] Liu, M., Seeder, S., and Li, H., "Analysis of E-Scooter trips and their temporal usage patterns," *Institute of Transportation Engineers. ITE Journal, 89*(6), 2019, pp. 44-49.

[20] Bloom, M. B., Noorzad, A., Lin, C., Little, M., Lee, E. Y., Margulies, D. R., and Torbati, S. S., "Standing electric scooter injuries: impact on a community," *The American Journal of Surgery, 221*(1), 2020, pp. 227-232.

[21] Austin Public Health, "Dockless Electric Scooter-Related Injuries Study," Austin Public Health, Austin, Texas, 2019.

[22] "Oregon Municipal Code," 1997, https://library.qcode.us/lib/port_orford_or/pub/municipal_code/item/title_12-chapter_12_20-12_20_120.

[23] Yates, K. M., *Protection of Rear Seat Occupants Using Finite Element Analysis*, Ph.D dissertation. Virginia Tech, 2020.

[24] Farley, K. X., Aizpuru, M., Wilson, J. M., Daly, C. A., Xerogeanes, J., Gottschalk, M. B., and Wagner, E. R., 2020, "Estimated incidence of electric scooter injuries in the US from 2014 to 2019," *JAMA Network Open, 3*(8), pp. e2014500-e2014500.

[25] 73 FR 40016, Docket No. NHTSA-2006-26555. https://www.federalregister.gov/documents/2008/07/11/E8-15620/consumer-information-new-car-assessment-program

[26] Stander, N. B., A.; Roux, W.; Liebold, K.; Eggleston, T.; Goel, T.; Craig, K., "LS-OPT® User's Manual, A Design Optimization and Probabilistic Analysis Tool for The Engineering Analyst," LSTC, Livermore, CA, 2020.

[27] R., F., *Statistical Methods for Research Workers*, Oliver and Boyd, Edinburgh, UK, 1925.

[28] Szucs, D., and Ioannidis, J. P., "When null hypothesis significance testing is unsuitable for research: a reassessment," *Frontiers in Human Neuroscience, 11*, 2017, p. 390.

[29] Chontos, R., Grindle, D., Untaroiu, A., Doerzaph, Z., and Untaroiu, C., "A Numerical Investigation of Rider Injury Risks During Falls Caused by E-scooter–Stopper Impacts," *ASME Journal of Biomechanical Engineering, 145*(10), 2023, 101006.

[30] Wei, W., Petit, Y., Arnoux, P.-J., and Bailly, N., "Head-ground impact conditions and helmet performance in E-scooter falls," *Accident Analysis & Prevention, 181*, 2023, p. 106935.

[31] Simms, C., and Wood, D., *Pedestrian and cyclist impact: a biomechanical perspective*, Springer Science & Business Media, 2009.

[32] Untaroiu, C. D., Pak, W., Meng, Y., Schap, J., Koya, B., and Gayzik, S., "A finite element model of a midsize male for simulating pedestrian accidents," *Journal of Biomechanical Engineering, 140*(1), 2018.

[33] Grindle, D., Pak, W., Guleyupoglu, B., Koya, B., Gayzik, F. S., Song, E., and Untaroiu, C., "A detailed finite element model of a mid-sized male for the investigation of traffic pedestrian accidents," *Proc Inst Mech Eng H, 235*(3), 2021, pp. 300-313.

[34] Pak, W., Grindle, D., and Untaroiu, C., "The influence of gait stance and vehicle type on pedestrian kinematics and injury risk," *Journal of Biomechanical Engineering, 143*(10), 2021.

[35] Chontos, R., Grindle, D., Untaroiu, A., Doerzaph, Z., and Untaroiu, C., "A Finite Element Model of an Electric Scooter for Simulating Traffic Accidents," *Proc. International Design Engineering Technical Conferences and Computers and Information in Engineering Conference, American Society of Mechanical Engineers*, 2022, p. V001T001A003.

[36] Schwartz, D., Guleyupoglu, B., Koya, B., Stitzel, J. D., and Gayzik, F. S., "Development of a computationally efficient full human body finite element model," *Traffic Injury Prevention, 16*(sup1), 2015, pp. S49-S56.

[37] Novotny, A. J., *Improving E-Scooter Safety: Deployment Policy Recommendations, Design Optimization, and Training Development*, Ph.D. dissertation. Virginia Tech, 2023.

[38] Klug, C., Feist, F., Raffler, M., Sinz, W., Petit, P., Ellway, J., and van Ratingen, M., "Development of a procedure to compare kinematics of human body models for pedestrian simulations," Presented at International Research Council on the Biomechanics of Injury: IRCOBI 2017 - Antwerp, Belgium, 2017.

[39] Peng, Y., Yang, J., Deck, C., and Willinger, R., "Finite element modeling of crash test behavior for windshield laminated glass," *International Journal of Impact Engineering, 57*, 2013, pp. 27-35.

[40] Lef, C., and Dolange, G., *Understanding Lower Leg Injury in Offset Frontal Crash: A Multivariate Analysis*. Master's thesis. KTH Royal Institute of Technology, Stockholm, Sweden, 2015.

[41] Störmann, P., Klug, A., Nau, C., Verboket, R. D., Leiblein, M., Müller, D., Schweigkofler, U., Hoffmann, R., Marzi, I., and Lustenberger, T., "Characteristics and injury patterns in electric-scooter related accidents—a prospective two-center report from Germany," *Journal of Clinical Medicine, 9*(5), 2020, p. 1569.

[42] Decker, W., Koya, B., Pak, W., Untaroiu, C. D., and Gayzik, F. S., "Evaluation of finite element human body models for use in a standardized protocol for pedestrian safety assessment," *Traffic Injury Prevention, 20*(sup2), 2019, pp. S32-S36.

[43] Song, E., Uriot, J., Potier, P., Dubois, D., Petit, P., Trosseille, X., and Douard, R. Reference PMHS Tests to Assess Whole-Body Pedestrian Impact Using a Simplified Generic Vehicle Front-End (IRC-17-25). Presented at IRCOBI Conference, 2017. https://www.ircobi.org/wordpress/downloads/irc17/pdf-files/25.pdf

Appendix. Additional Result Tables for E-scooter Stopper Impacts/Injury

Table 3. DOE Results – E-scooter Stopper Impacts/Probability of Serious Injury: Whole Body and Regional Injuries

Case	Approach angle	Stopper height (mm)	Velocity (m/s)	RIM	HIC	Nij	Chest	Femur
1	90	52	3.20	0.496	0.173	0.271	0.152	0.014
2	60	52	3.20	0.961	0.946	0.257	0.001	0.02
3	45	52	3.20	0.974	0.97	0.117	0.001	0.024
4	30	52	3.20	0.08	0	0.063	0	0.018
5	90	101	3.20	0.86	0.782	0.33	0.026	0.015
6	60	101	3.20	0.645	0.426	0.368	0.003	0.018
7	45	101	3.20	0.145	0.001	0.124	0.001	0.022
8	30	101	3.20	0.101	0	0.081	0	0.019
9	90	152	3.20	1	0.999	0.645	0.149	0.015
10	60	152	3.20	0.083	0	0.066	0	0.018
11	45	152	3.20	0.112	0	0.091	0	0.023
12	30	152	3.20	0.087	0	0.07	0	0.017
13	90	52	4.48	0.772	0.995	0.461	0.112	0.014
14	60	52	4.48	0.738	0.165	0.667	0.004	0.054
15	45	52	4.48	0.451	0.177	0.323	0.001	0.014
16	30	52	4.48	0.815	0.343	0.661	0.136	0.041
17	90	101	4.48	1	1	0.379	0.295	0.024
18	60	101	4.48	0.348	0.22	0.142	0.001	0.024
19	45	101	4.48	0.7	0.545	0.326	0.003	0.018
20	30	101	4.48	0.975	0.961	0.354	0.002	0.035
21	90	152	4.48	0.966	0.67	0.845	0.328	0.028
22	60	152	4.48	0.088	0	0.071	0	0.018
23	45	152	4.48	0.111	0	0.09	0	0.022
24	30	152	4.48	0.09	0	0.073	0	0.019
25	90	52	11.16	1	1	0.499	0.176	0.036
26	60	52	11.16	1	0.999	0.234	0.001	0.022
27	45	52	11.16	0.087	0	0.07	0	0.018
28	30	52	11.16	0.109	0	0.086	0	0.025
29	90	101	11.16	1	0.999	0.967	0.001	0.029
30	60	101	11.16	0.999	0.994	0.813	0	0.036
31	45	101	11.16	0.122	0	0.105	0	0.019
32	30	101	11.16	0.108	0	0.093	0	0.016
33	90	152	11.16	0.999	0.97	0.94	0.216	0.025
34	60	152	11.16	0.249	0.156	0.092	0	0.021
35	45	152	11.16	0.086	0	0.072	0	0.015
36	30	152	11.16	0.093	0	0.072	0.001	0.217

Table 4. E-scooter Stopper Impacts/Risk of Serious Injury for Head-on Impact Simulations

	Arm Activation	RIM	HIC	Nij	Chest	Femur
Case I $(90°, 52\ mm, 3.2\ m/s)$	No	0.49	0.17	0.27	0.15	0.01
	Yes	0.88	0.85	0.16	0.001	0.01
Case II $(90°, 101\ mm, 3.2\ m/s)$	No	0.86	0.78	0.33	0.03	0.01
	Yes	0.12	0	0.09	0.001	0.03
Case III $(90°, 152\ mm, 3.2\ m/s)$	No	1	0.99	0.64	0.15	0.01
	Yes	0.80	0.75	0.20	0	0.02
Case IV $(90°, 52\ mm, 4.48\ m/s)$	No	0.77	0.51	0.46	0.11	0.01
	Yes	0.91	0.84	0.28	0.24	0.03
Case V $(90°, 101\ mm, 4.48\ m/s)$	No	1	1	0.37	0.295	0.02
	Yes	0.76	0.68	0.24	0.01	0.04
Case VI $(90°, 152\ mm, 4.48\ m/s)$	No	0.96	0.67	0.84	0.33	0.03
	Yes	0.93	0.89	0.42	0.01	0.02
Case VII $(90°, 52\ mm, 11.2\ m/s)$	No	1	1	0.49	0.17	0.04
	Yes	1	1	0.48	0.26	0.03
Case VIII $(90°, 101\ mm, 11.2\ m/s)$	No	1	0.99	0.96	0.001	0.03
	Yes	0.84	0.18	0.80	0.002	0.03
Case IX $(90°, 152\ mm, 11.2\ m/s)$	No	0.99	0.97	0.94	0.22	0.03
	Yes	0.43	0.003	0.40	0.02	0.03

Table 5. E-scooter Stopper Impacts/Correlation Coefficients between Impact Speed and Injury Risk (No Arm Activation Cases)

	RIM	HIC	Nij	Chest	Femur
Case A $(90°, 52\ mm)$	0.91	0.96	0.74	0.68	0.99
Case B $(60°, 52\ mm)$	0.49	0.41	-0.40	-0.50	-0.31
Case C $(45°, 52\ mm)$	-0.89	-0.75	-0.52	-0.99	-0.29
Case D $(30°, 52\ mm)$	-0.33	-0.36	-0.33	-0.36	-0.05
Case E $(90°, 101\ mm)$	0.62	0.62	0.99	-0.43	0.88
Case F $(60°, 101\ mm)$	0.81	0.92	0.88	-0.78	0.98
Case G $(45°, 101\ mm)$	-0.40	-0.36	-0.43	-0.49	-0.49
Case H $(30°, 101\ mm)$	-0.36	-0.36	-0.34	-0.29	-0.46
Case I $(90°, 152\ mm)$	0.34	0.29	0.84	0.01	0.43
Case J $(60°, 152\ mm)$	0.99	0.99	1	0.98	1
Case K $(45°, 152\ mm)$	-0.99	0.98	-0.99	0.93	-0.99
Case L $(30°, 152\ mm)$	0.88	0.98	0.31	0.99	0.99
Overall	-0.03	0.066	0.121	-0.06	0.263